



ISSN: 2278 – 0211 (Online)

An Efficient Numerical Technique To Simulate The Propeller Hull Interaction

L Broberg

Ph.D in Mathematics, Chalmers University, Sweden
Director at FLOWTECH International AB, Sweden

M. Orych

Ph.D. student , Department of Shipping and Marine Technology,
Chalmers University Sweden
Project manager at FLOWTECH International AB, Sweden

Abstract:

The paper presents a technique where the propellers are modelled by a lifting line method that is tightly integrated with the RANS solver in SHIPFLOW. The effect of the propeller is taken into account by a force field computed by the lifting line method using the current velocity field. This results in an iterative procedure that is handled automatically by the program. The propeller is embedded in an cylindrical grid and the interaction with the surrounding grids for the hull and appendages are managed by the overlapping grid capability of solver. This results in an efficient method to predict the propeller hull interaction in terms of speed and accuracy for both conventional ships and ships equipped with energy saving devices. The computation can be performed at model scale and the results evaluated at full scale by extrapolation methods. The open water and resistance simulations required for the scaling is automated. It is also possible to carry out the simulation directly at full scale.

A validation of the method is presented with comparisons of resistance, open water test and self propulsion simulations at model scale. Extrapolated results and results from computations at full scale Reynolds number are compared with full scale data.

1.Introduction

The propeller modelling in SHIPFLOW has focused on propeller hull interaction. The original work was carried out in the late 1980 [1,2]. This was the first time a RANS solver was coupled with an external potential flow propeller analysis program to compute the propeller hull interaction of a three dimensional ship model. The results from these developments showed promising results for the technique to model the flow with coupled RANS and potential flow propeller methods. The use was at this time limited by computer resources and method did not come into practical use until the early 2000 when there had been a significant improvements of computer resources and accuracy of the RANS methods [3,4].

Some recent applications with SHIPFLOW are the work on hull/propeller/rudder optimizations [5], confined water effects [6], ship-to-ship interaction [6] and on energy saving devices [7].

This paper describes the procedures and methods in more detail and shows results from validation of the method for a container ship test case.

2.Computational Method

2.1.Flow Solvers

Computations are performed with SHIPFLOW developed at FLOWTECH International AB. There are three kinds of flow solvers in SHIPFLOW. XCHAP is a RANS solver for steady incompressible flow, XPAN a potential flow solver and XBOUND is an integral method for thin boundary layers. The solvers can be used separately or in combination depending on the needs.

The zonal approach is an efficient technique for many applications. The methods are in this case applied in a sequence. The free surface and the dynamic trim are first computed by XPAN, thereafter the boundary layer on the fore body by XBOUND and finally the flow around the stern and in the wake by XCHAP. Alternatively, the more general global approach can be used where the complete flow domain is computed by XCHAP.

2.1.1.Potential flow solver

The potential flow method XPAN is a non-linear Rankine source panel method [8]. It uses higher order panels and singularity distributions and a non-linear free surface boundary conditions.

The method can handle lift and induced drag by adding dipoles to the lifting surfaces and trailing wake. A Kutta condition is applied to find the strength of the bound circulation. Dynamic sinkage and trim are computed during the iterative procedure for the non-linear free surface boundary condition. During each iteration the ship is repositioned and the panellization of the hull and free surface is regenerated.

2.1.2. Boundary Layer Method

XBOUND is a first order integral method [9]. It computes the boundary layer along potential flow streamlines. The flow can be laminar or turbulent. The method includes a model for the transition from laminar to turbulent flow.

2.1.3. RANS solver

XCHAP solves the steady incompressible Reynolds Average Navier-Stokes equations. There are two available turbulence models the k- ω SST [10] and the Explicit Algebraic Stress Model EASM [11,12]. The EASM takes the non-isotropy into account using algebraic expressions for the Reynolds stresses containing non-linear terms in the mean strain and rotation rates. The model is a good compromise between performance and the ability to predict the important vortex flow in the stern wake and is therefore the standard model in the program. No wall functions are used and the equations are integrated down to the wall.

The entire system of Navier-Stokes and continuity equations in conservation form including the turbulence equations can be represented in a generic way by

$$\frac{\partial Q}{\partial t} + \frac{\partial F}{\partial x} + \frac{\partial G}{\partial y} + \frac{\partial H}{\partial z} = R \quad (1)$$

where Q , F , G , H , R are column vectors. The column vectors on the left side of equation (1), given by F , G , and H represent fluxes, while Q represents primitive variables. The flux vectors of the linearised equations (1) are split into convective and viscous fluxes. On the right side, vector R , represents the source term, which in our case can be body, inertia or gravity forces.

The partial differential equations (1) are discretized to algebraic equations with the Finite Volume Method (FVM). The averaged values in each cell volume surrounding the centres are calculated from face fluxes. The flux entering a volume through a face equals to the flux leaving the adjacent volume through that face and therefore the method is conservative.

For the convective fluxes the approximate Riemann solver of Roe [13] is used, while for the diffusive fluxes central differences around the cell face centres are used. The second order accuracy is obtained with the explicit correction [14]. Flux limiters based on [15] are incorporated into the discretization scheme in order to avoid wiggles in the solution that may occur due to not monotonicity-preserving schemes such as central or fully upwind.

The discrete coupled equations are solved with the Alternating Direction Implicit (ADI) method. The system matrix contains the first order Roe convective terms and the second order diffusive terms. The second order convective correction is treated as an explicit defect correction. The resulting system matrix is a block tri-diagonal system. A local artificial time step based on the Courant–Friedrichs–Lewy number (CFL) and the von Neumann numbers is applied in all directions except the implicit.

The boundary conditions in XCHAP are inlet, outlet, slip, no-slip and interior. Velocity and turbulence quantities are prescribed at the inlet while the pressure gradient normal to the inlet plane is set to zero. The gradient normal to the outlet plane is set to zero for the velocity and turbulence quantities and the outlet while the pressure is set to zero. The slip condition is normally used for simulating symmetry conditions at flat boundaries. In this case the normal velocity component and all the normal gradient of all the other quantities are zero. The slip boundary condition is applied for solid walls thus the velocity, the turbulent kinetic energy and the normal pressure gradient are set to zero. The turbulent dissipation rate is treated according to [16]. The flow field is obtain by interpolation from other grid components at interior boundaries. Mixed boundary conditions on boundary surfaces are also available for example inflow/outflow which are typically used at the outer boundary of an O-O type of grid and no-slip/slip which are used for a H-O type of grid for ship hulls. Two layers of ghost cells are used at the boundaries. For a Dirichlet conditions the value at the boundary is extrapolated with second order accuracy to the ghost cells. The normal flux is specified at a Neumann boundary and used to linearly extrapolate to the ghost cells. The values of the variables are updated in each ADI

iteration. A special stencil is used along the boundaries to maintain the second order of the diffusion.

XCHAP use structured grids. A single block grid is typically used for a bare hull case. Multi-block structured or overlapping grids are used for more complex geometries for example appended hulls, see Figure 1. The solver is flexible in terms of H/C/O grid topologies, it can handle grid point and line singularities at the boundary surfaces, folded and periodic grids.

All cells in the overlapping grid needs to be classified as fluid, outside or interpolation cells. The interpolation stencil is also required for the interpolation cells. XCHAP has an automatic algorithm for the cell classification:

- Calculate the local distance function in every node point. The distance function represents the distance from a point to the nearest point on a part of the fluid domain boundary represented by the grid.
- Classify all cells as fluid or interpolation cells. Cells that are overlapped by cells in other grids are detected. The cell closest to the fluid domain boundary, measured by the local distance function, is classified as a fluid cell while the remaining cells are market as interpolation cells.
- All cells that are intersected by a physical boundary (boundary cell face) are classified as being potentially outside the fluid domain if its cell centre is outside of the boundary.
- All neighbouring cells of an outside cell are recursively classified. If a neighbour is overlapped by the grid that made the original intersection in point 3 it is not outside, otherwise the line from the point to the neighbour is tested for intersection with the fluid domain boundary. If the number of intersections is odd the neighbour is not outside and if it is even its is outside and the recursion continues.

A special type of grid component is the local refinement grid, where a refinement grid is created from a sub-division of another grid component.

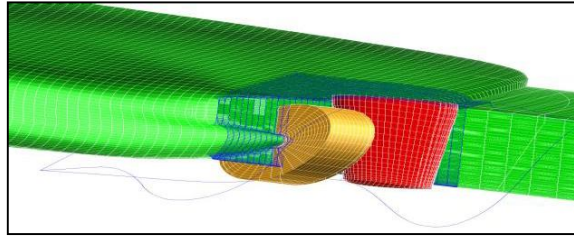


Figure 1: Overlapping grid; hull, refinement, propeller, rudder

2.2. Modelling Of The Propeller

To simulate the effect of the propeller, body forces are introduced in a cylindrical component grid in the overlapping grid. When the flow passes through the propeller its linear and angular momentum increases as if it had passed a propeller of infinite number of blades. The forces vary in space but are independent of time and therefore approximating a propeller induced steady flow.

In SHIPFLOW the body forces can be computed with a built in lifting line propeller analysis program. The axial and tangential force components fb_x and fb_t , respectively, are related to the local thrust and torque which depends on the blade circulation. The circulation varies in both the radial and circumferential directions of the propeller disk. From the Kutta-Joukowski theorem the forces per volume unit can be written as

$$\begin{aligned} fb_x &= \frac{ZG_L}{\Delta x_p} \left(\frac{\pi}{J} + \frac{u_{TH} - u_T}{U_0 r} \right) \\ fb_t &= \frac{ZG_L}{\Delta x_p r} \left(\frac{V_A}{U_0} + \frac{u_A}{U_0} \right) \end{aligned} \quad (2)$$

where V_A , u_{TH} , u_A and u_T are the local values of axial and tangential inflow and propeller induced velocities. J is the advanced ratio based on the ship speed U_0 . Δx_p is the length of the cylindrical domain where the body forces are applied. Z is the number of blades of the equivalent finite bladed propeller. G_L is the dimensionless local blade circulation.

The induced velocities of a propeller with finite number of blades are obtained using Goldstein's kappa theory. The lift coefficient of the blades is expressed as

$$C_L = C_{L0} + \frac{\partial C_L}{\partial \alpha} \alpha \quad (3)$$

where C_{L0} is calculated from two-dimensional profile theory and corrected for lifting surface effects. The blade geometry is specified in term of length, camber, thickness and pitch which are given at different radial positions. α is the angle of attack. The lift coefficient slope is approximated by

$$\frac{\partial C_L}{\partial \alpha} = 2\pi k_f \quad (4)$$

where k_f is the camber correction caused by lifting surface effects. The difference between the geometric and hydrodynamic pitch angles gives the local values of α . The circulation and the body forces can be derived from (3).

The frictional drag of the blade is calculated in an approximate way by an empirical formula for the blade section drag.

The computation of the body forces are embedded in an iterative procedure where first the current approximation of the velocity field is extracted at a representative propeller plane. The effective wake is thereafter obtained by subtracting the induced propeller wake. This is the responsibility of the propeller code and is computed by the circulation from the previous iteration in the lifting line method. The new circulation, forces and torques are computed in the effective wake. Thereafter the forces are distributed over the volume cells in the cylindrical grid. The body forces are added to the right hand side of the flow equations. This can be done in an active mode, where the flow equations are solved in the cylindrical component grid. Alternatively, the body forces can be interpolated to the grid embedding the cylindrical grid. In this passive mode, the flow equations are not solved in the cylindrical grid instead the forces are added to the right hand side of the equations in the embedding grid. The body forces are updated every tenth iteration in XCHAP. At convergence the total wake computed by XCHAP and the lifting line method should match in the selected propeller plane.

External propeller analysis codes can be interfaced to SHIPFLOW and used in a similar way as the built-in lifting line method, see for example [5].

2.3. Scaling

The computations can be carried out directly at full scale or at model scale and then extrapolated to ship scale. In the latter case the results need to be scaled to the ship scale. In case of the self propulsion simulation SHIPFLOW can apply the ITTC78 procedure

for the scaling based on resistance and open water results from simulations or experiment. The results, for example efficiencies, from the simulation will be presented in a similar way to experimental results. These results are of importance for the evaluation of the propeller performance. However, the scaling can be problematic in particular for appended hulls, for example with energy saving devices, and the possibility to compute directly at full scale becomes important.

3. Validation

The self propulsion simulation with SHIPFLOW is demonstrated in this paper by a validation carried out for the SSNAME workshops hosted by MARIC in Shanghai 2010-2012.

The hull used during the workshops is a 4000 TEU container ship of the length LPP=260 m and with a block coefficient $CB=0.64$. The model was tested at MARIC and at Shanghai Jiaotong University.

3.1. Resistance

A grid variation study was carried out to gain knowledge for the modelling and grid

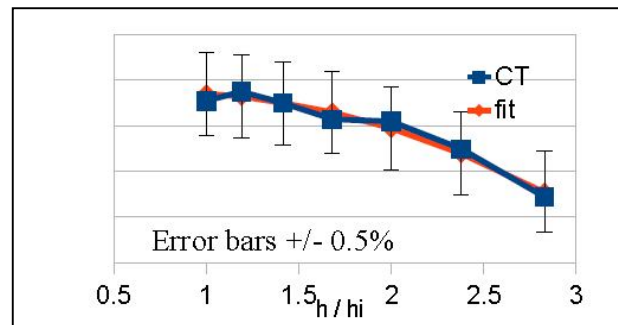


Figure 2: Grid refinement

generation of the model. A sequence of seven grids ranging from approximately 400000 to 9000000 cells with a refinement ratio of $\sqrt[3]{2}$ were created. The total resistance as a function of the refinement is shown in Figure 2 below. The values of the coefficient is not presented, instead error bars of 0.5% is used to indicate the relative differences between grids.

More thorough investigations on errors and uncertainties estimations using XCHAP for similar cases can be found in for example [3,6].

The resistance was computed at six speeds using the global approach in SHIPFLOW. The wave resistance was computed by the potential flow module XPAN. The number of panels was adjusted to the Froude number such that the number of panels per wave length was kept at 25 for all speeds. The computational domain was kept at a distance of two fundamental wave lengths or at least one ship length aft of the ship and a half ship length upstream. The grid domain used for XCHAP was ranging from 0.5 to 0.8 ship length upstream and downstream of the ship, respectively. The outer boundary was located at a radius of 2 ship length from the centre axis. The number of cells were 70x100x394 in circumferential, normal and longitudinal directions, respectively. The height of the cell closest to the hull surface were located at a distance of $y^+=1$ at all speeds.

The total resistance curve is shown in Figure 3. The difference in CT between experiments and the computations were in the range from 2.5 to 4.5 percent.

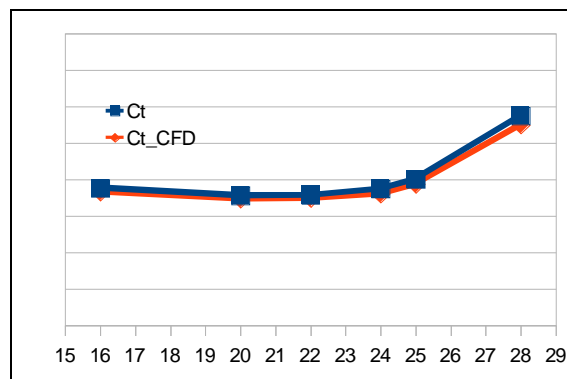


Figure 3: Resistance curve

The nominal axial wake from the experiments and computations are shown in Figure 4. The results are taken from the finest grid use in the grid refinement study. The shaft of the measurement equipment was included in the hull definition.

3.2. Open Water

The open water characteristics are required in order to make the full scale extrapolation using the ITTC78 procedure. SHIPFLOW can automatically compute an open water simulation for a sequence of advance ratios. The program creates a box grid with inflow, outflow and slip boundaries to model the water tunnel. The box grid is stretch appropriately to resolve the relatively small cylindrical propeller grid that is positioned in the centre, Figure 5. The relatively simple inflow allows for a grid of about 370000 cells.

The program runs the simulation for the different advance ratios and creates a table with the resulting thrust, torque coefficients and open water efficiency.

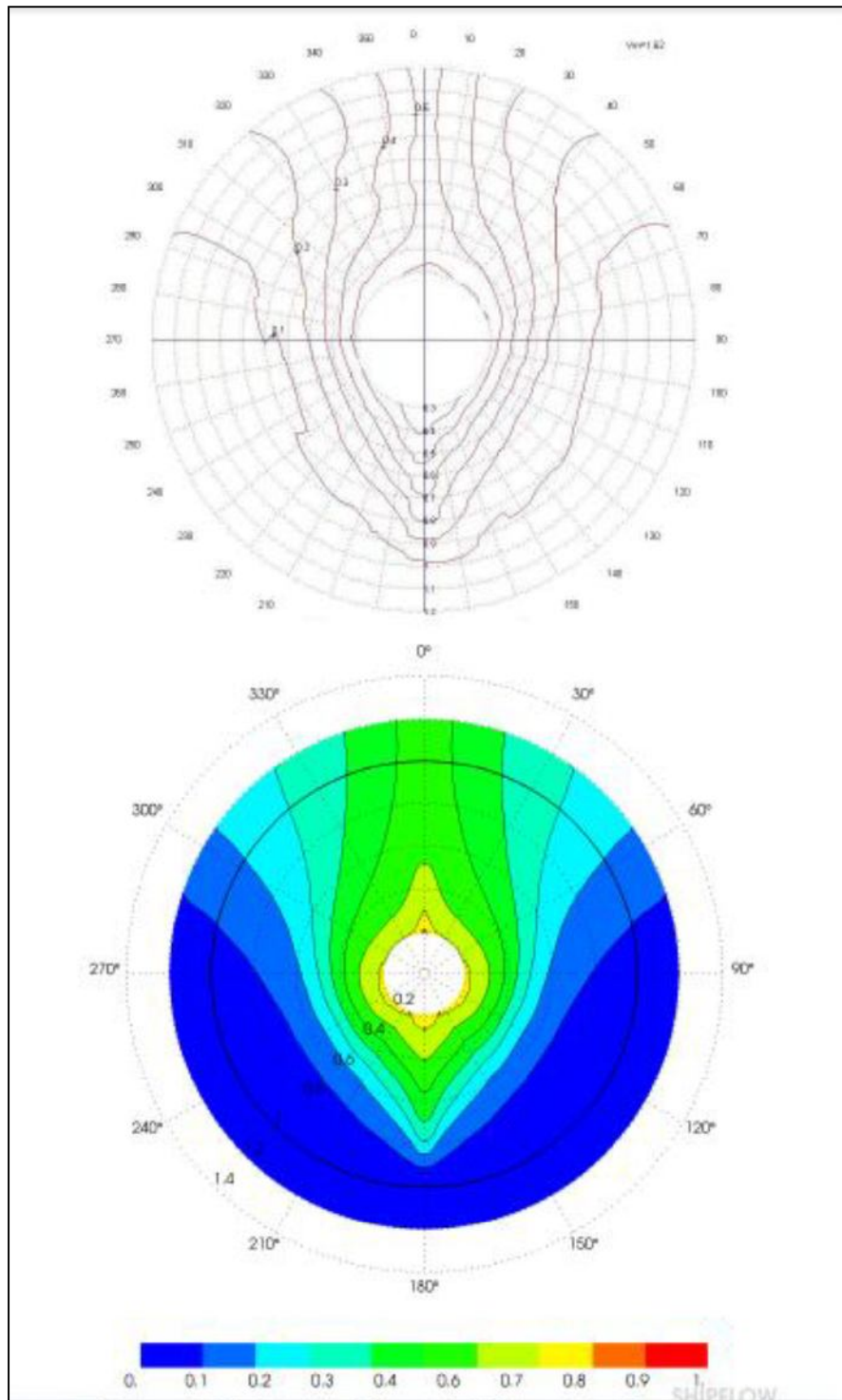


Figure 4: Axial wake. Top - EFD, Bottom - CFD

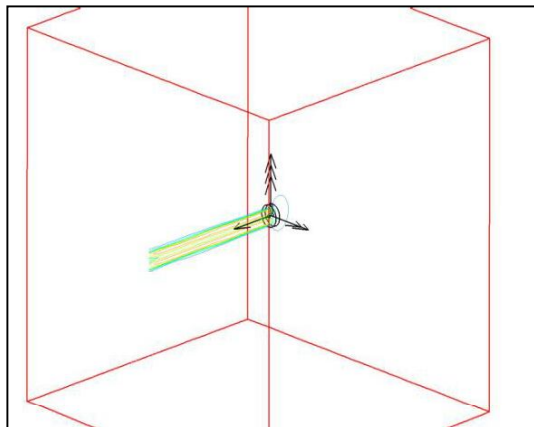


Figure 5: Open water simulation. Box and propeller grid.

The propeller used in the self propulsion is a conventional five bladed stock propeller. The results from the simulation is compared to the experimental results in Figure 6. The computations corresponds well to the experiments around the design point, but deviates for lower and higher advance ratios. This behaviour is known for the lifting line model of the propeller.

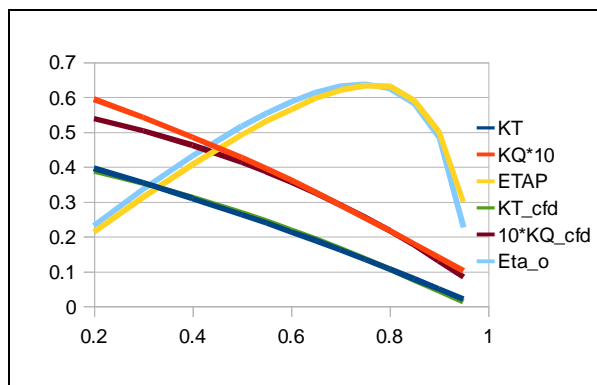


Figure 6: Open water results

3.3. Self Propulsion

The resistance and self propulsion simulations were performed for a speed of 25 knots and at one draft in model scale.

It was assumed that the effect from the free surface was negligible on the wake flow and therefore approximated by a symmetry plane. The speed of the propeller was automatically adjusted during the self propulsion simulation such that the propeller thrust balanced the resistance of the hull corrected for the towing force. The towing force was

computed according to the ITTC78 procedure and include the model-ship correlation and roughness allowance.

The zonal approach was applied for the simulation. The inflow was located at midship and the outlet at 0.8 ship length downstream. The outer radius was located at two ship length from the centre axis. The hull grid consisted of 2.2 million cells covering both sides of the model. Including the additional overlapping grid components, the propeller grid, the rudder grid and a local refinement grid in the stern the total number of cells were 3.4 million. The overlapping grid is illustrated in Figure 1.

The predicted delivered power at ship scale was 0.9% lower in the computations than in the experiments using the ITTC78 extrapolation. Similarly the propeller speed was 1.1% lower in the computations. The computation performed at full scale gave a 7% lower value of the delivered power compared to the extrapolated results.

6. Conclusion

A method to predict the propeller hull interaction has been described in the paper. The propeller is modelled with a lifting line method and integrated with a RANS solver using overlapping grids. It can be concluded that the overlapping grid provides an efficient environment to implement and execute the interfacing between the RANS solver and the external propeller program.

The method was applied for a 4000 TEU container ship. From these computations the following can be concluded:

- A grid dependence study indicated a grid convergence of the integrated total resistance. Some scatter in the result were noted.
- The power prediction showed a reasonable agreement with the experiments.
- The open water simulation agrees well with experiments. Some deviations were noted for of design points.
- The delivered power compares well at ship scale after applying the ITTC78 extrapolation procedure.
- Direct simulation at ship scale gave larger deviation between computation and experiments based on the ITTC78 procedure than the results based on computation at model scale.

7.Acknowledgement

The authors which to thank Marine Design & Research Institute of China (MARIC) for the permission to use their test results in the paper.

8.Reference

1. ZHANG, D.-H., 'Numerical Calculation of Ship Stern/Propeller Flow', PhD Thesis, Chalmers University of Technology, Gothenburg, 1990.
2. ZHANG, D.-H., Broberg, L., Larsson, L., Dyne, G., 'A Method for Computing Stern Flows with an Operating Propeller', Transactions, Royal Institution of Naval Architects, Vol. 143, 1991.
3. LARSSON, L., STERN, F., VISONNEAU, M. (editors), 'Gothenburg 2010. A Workshop on Numerical Ship Hydrodynamics', Proceedings Vol. II, 2010.
4. LARSSON, L., STERN, F., VISONNEAU, M., 'CFD In Ship Hydrodynamics – Results of the Gothenburg 2010 Workshop', Proceedings of Marine 2011 Lisbon, 2011.
5. Han, K.-J., 'Numerical optimization of Hull / Propeller / Rudder Configurations', Ph.D. Thesis, Chalmers University of Technology, Sweden, 2008.
6. Zou, L., 'CFD Predictions Including Verification and Validation of Hydrodynamic Forces and Moments on Ships in Restricted Waters', Ph.D. Thesis, Chalmers University of Technology, Sweden, 2012.
7. Kim, K., Leer-Anderson, M., Werner, S., Orych, M., Choi, Y., 'Hydrodynamic Optimization of Pre-swirl Stator by CFD and Model Testing', 29th Symposium on Naval Hydrodynamics, Gothenburg, Sweden, 2012.
8. JANSON, C.-E., 'Potential Flow Panel Method for the Calculation of Free-Surface Flows with Lift', Ph.D. Thesis, Chalmers University of Technology, 1997.
9. BROBERG, L., et. al., 'SHIPFLOW Users Manual', FLOWTECH International AB, Sweden, 2011
10. MENTER, F.R., 'Zonal Two Equation k-w Turbulence Models for Aerodynamic Flows', 24th Fluid Dynamics Conference, Orlando, AIAA paper-93-2906, 1993
11. GATSKI, T., SPEZIALE, C.G., 'On Explicit Algebraic Stress Models for Complex Turbulent Flows', Journal of Fluid Mechanics, 254, 59-78, 1993
12. DENG, G.B., Queutey, P., Visonneau, M., 'Three Dimensional Flow Computation with Reynolds Stress and Algebraic Stress Models', Engineering Turbulence Modelling and Experiments 6, Rodi, W., Mulas, M., Editors, ELSEVIER, 389-398, 2005
13. HELLSTEN, A., LAINE, S., 'Extension of the k-w SST model for Flows over Rough Surfaces', AIAA-97-3577, 252-260, 1997

14. ROE, P. L., 'Approximate Riemann Solvers, Parameter Vectors, and Difference Schemes', Journal of Computational Physics, Vol. 135, No. 2, pp. 250-258, 1997.
15. CHAKRAVARTHY, S. & OSHER, S., 'A New Class of High Accuracy TVD Schemes for Hyperbolic Conservation Laws', AIAA paper-85-0363, 1985.
16. LEONARD, B. P., 'The ULTIMATE conservative difference scheme applied to unsteady one-dimensional advection'. Computer Methods in Applied Mechanics and Engineering, 88, 17-74, 1991.